Aromatic Carboxylate Superhalogens and Multiply Charged Anions

Mark Enlow*,† and J. V. Ortiz‡

Department of Chemistry, University of New Mexico, Albuquerque, New Mexico 87131, and Department of Chemistry, Kansas State University, Manhattan, Kansas 66506

Received: January 16, 2002; In Final Form: March 18, 2002

Ab initio calculations employing electron propagator theory and many-body perturbation theory show that the benzoate anion is a superhalide with an electron detachment energy in excess of 4.4 eV. Final states associated with vertical electron detachment energies of the benzoate anion are reordered by correlation effects, and the holes associated with the lowest neutral states thereby have O-centered σ character instead of ring-centered π character. Geometry optimizations on the dianions produced by attaching two carboxylate groups to the benzene ring arrive at planar structures for the para and meta isomers, but in the ortho isomer, a C_2 structure with twisted OCO groups is found. The most stable isomer is para, and the least stable is ortho. The lowest vertical detachment energies are at least 1.4 eV for the para and meta isomers, but the estimate for the ortho isomer is 0.8 eV. Corresponding Dyson orbitals exhibit ring-centered π character. Attempts to find bound trianions with three carboxylate groups failed. In fluorinated compounds, the carboxylate groups rotate so that they are perpendicular to the ring planes. These compounds possess higher electron binding energies. The associated Dyson orbitals are delocalized over the ring, F, and carboxylate regions, and antibonding phase relationships are obtained between ring π and substituent lobes.

Introduction

Among the most vigorous trends in anion chemistry and physics are efforts to discover superhalogens and multiply charged anions that are stable in the gas phase. Superhalogens are molecules with electron affinities that are larger than those of the halogen atoms.[2,3] These species may be useful in the oxidation of molecules with high ionization potentials, thus leading to new classes of ionic compounds. Among these ionically bound substances are organic metals and superconductors. Many superhalogens have been identified through calculations or experimental techniques. The most prominent examples include molecules with the formula MX_{k+1}, where M is a main group or transition-metal element, X is a halogen, and k is the maximum oxidation state of M. Superhalides such as BF_4^-, $AlCl_4^-$, and AsF_6^- are commonly found fragments in gas-phase molecules and in crystalline solids.

Multiply charged anions that are stable with respect to electron loss in the gas phase have been identified by theory and experiment as well.[1] Many of the species familiar to chemistry students, such as sulfate and phosphate anions, are not stable in the absence of a surrounding matrix of counterions or solvent molecules. Multiply charged anions that are intrinsically stable are most often built from metallic atoms complexed to halogen, oxygen, or sulfur atoms. Examples include $AlkX_3^{2-}$ (Alk = alkali metal, X = F, Cl),[4] AeF_4^{2-} (Ae = alkaline earth),[4] and MF_{k+2}^{2-} (M = transition-metal atom and k = maximum oxidation state of M).[5] More highly charged anions with the formula $M_mX_{mk+n}^{n-}$ have been discussed.[6] All of these patterns are based on ionic bonding and the delocalization of excess negative charge over several electronegative centers.

Another aspect of the search for multiply charged anions concerns carbon clusters. Dianions of carbon clusters with at least seven nuclei have been found in the mass spectra of sputtered graphite and other similar sources. Theoretical investigations have suggested that bound anions may exhibit linear or nonlinear structures, depending on the number of nuclei.[7−9] A set of structural motifs, such as alternating single and triple bonds, may be employed to delocalize excess negative charge.[10]

Thus far, the search for superhalogens and intrinsically stable, multiply charged anions has often ignored the most common structural motifs of organic chemistry. The design of organic charge-transfer salts and other materials depending on highly electronegative organic species may be abetted by the identification of organic superhalogens and dianions. In this work, the juxtaposition of carboxylate groups with the benzene ring is investigated to identify superhalogens and intrinsically stable dianions and trianions. Because inorganic superhalogens often contain F atoms, we decided also to study the organic species in which H atoms were replaced by F atoms. This was considered a likely procedure for identifying anions with large electron detachment energies. Ab initio techniques incorporating electron correlation are applied.

Methods

Calculations were performed with a modified version of Gaussian 94.[11] Geometry optimizations were performed at the Hartree−Fock level of theory using the aug-cc-pVDZ[12,13] basis set with the most diffuse d orbitals omitted from the heavy atoms. The most diffuse set of d orbitals was found to have a minimal effect on the calculated results for these and similar systems and was omitted to reduce the disk requirements in the post-SCF procedures. Harmonic frequency calculations were then performed to ensure that a stationary geometry had been obtained. For the hydrogen-containing species, the geometry was then further refined with second-order many-body perturbation theory with the same basis set. Property calculations were

* Corresponding author. E-mail: menlow@ahpcc.unm.edu.
† University of New Mexico.
‡ Kansas State University.

10.1021/jp0201074 CCC: $22.00
Published on Web 05/01/2002

performed using this geometry. Symmetry constraints were imposed in all cases.

In some cases, vertical and adiabatic electron detachment energies were estimated by removing an electron from the system and performing an additional geometry optimization. The vertical electron detachment energy is the difference between the N electron system at its equilibrium geometry and the $N-1$ electron system at the same geometry. The adiabatic electron detachment energy is the difference between the N electron system at its equilibrium geometry and the $N-1$ electron system at its own equilibrium geometry.

Electron propagator calculations were performed in the OVGF[14,15] approximation using a semidirect algorithm[16,17] that takes advantage of abelian point-group symmetry. Only 1s core orbitals were omitted from the summations required by this approximation. The aug-cc-pVDZ basis with the most diffuse d orbitals omitted from the heavy atoms was used. Iterations on the Dyson equation were performed until the electron binding energies converged to within 0.00001 eV.

Dyson orbitals for an electron detachment from an N-electron state are defined by

$$\phi^{\text{Dyson}}(x_1) = \int \Psi^*_{N-1}(x_2, x_3, x_4, ..., x_N) \times \Psi_N(x_1, x_2, x_3, ..., x_N)\, dx_2\, dx_3\, dx_4 ... dx_N \quad (1)$$

Propagator programs report electron detachment energies and corresponding pole strengths, p, where

$$p = \int |\phi^{\text{Dyson}}_{(x_1)}|^2\, dx_1 \quad (2)$$

Normalized Dyson orbitals are depicted in plots generated with the program MOLDEN.[18] In the zeroth-order propagator, the results of Koopman's theorem are recovered, and the pole strengths equal unity. In the OVGF model, correlation contributions are included in the electron binding energies, and pole strengths may be less than unity. The closer to unity the pole strengths are, the greater the qualitative validity of Koopman's description of the electron detachment. Dyson orbitals remain proportional to canonical orbitals in the OVGF model.

Structures

$C_6H_5CO_2^-$. Optimizations on the benzoate anion produce a planar C_{2v} structure. This structure and the numbering scheme for its atoms is given in Figure 1a. A nonplanar C_{2v} structure with the CO_2 group perpendicular to the plane of the benzene ring is a transition state that lies 5.85 kcal/mol above the equilibrium geometry. Other structures with a rotated CO_2 group that retain the C_2 symmetry axis revert to the minimum conformation. Total energies for this and other structures and rotamers are summarized in Table 1.

Optimized bond lengths and angles shown in Table 2 are typical for compounds with benzene rings and carboxylate groups. A C−C single bond with an internuclear distance of 1.55 Å connects the ring to the carboxylate group. A somewhat long C−O bond (1.265 Å) and an O−C−C angle of 130° suggest that repulsions between negatively charged oxygens affect the structure somewhat.

***p*-$C_6H_4(CO_2)_2^{2-}$.** Optimization on the para isomer (Figure 1b) produces a D_{2h} minimum with bond lengths and angles that are given in Table 3. The structures of the ring and carboxylate groups are similar to those found in the benzoate anion. The C_{2v} structure with a single carboxylate perpendicular to the ring plane is a transition state that lies 5.63 kcal/mol (Table 1) above the D_{2h} geometry. Intermediate structures with a rotated carboxylate revert to the same minimum.

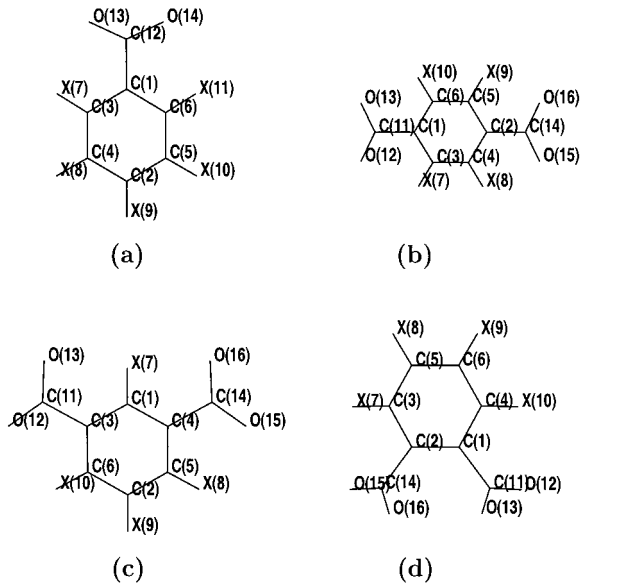

Figure 1. Numbering scheme and structural schematic for the species studied. X = H or F; (a) $C_6X_5CO_2^-$; (b)−(d) ortho, meta, and para $C_6X_4(CO_2)_2^{2-}$, respectively.

TABLE 1: Relative Energies (au) and Energy Differences (kcal/mol) of Selected Rotamers at the HF/aug-cc-pVDZ Level of Theory

structure	conformation	classification	E	ΔE
$C_6H_5CO_2^-$	planar C_{2v}	minimum	−417.81248	0
	nonplanar C_{2v}	transition state	−417.80315	+5.85
p-$C_6H_4(CO_2)_2^{2-}$	planar D_{2h}	minimum	−604.81950	0
	nonplanar C_{2v}	transition state	−604.81052	+5.63
m-$C_6H_4(CO_2)_2^{2-}$	planar C_{2v}	minimum	−604.81149	0
o-$C_6H_4(CO_2)_2^{2-}$	planar C_{2v}	transition state	−604.74864	+14.9
	nonplanar C_{2v}	transition state	−604.76765	+3.0
	twisted C_2	minimum	−604.77236	0
$C_6F_5CO_2^-$	planar C_{2v}	transition state	−912.08037	+5.3
	nonplanar C_{2v}	minimum	−912.08879	0
p-$C_6F_4(CO_2)_2^{2-}$	nonplanar D_{2h}	minimum	−1000.24889	0
m-$C_6F_4(CO_2)_2^{2-}$	nonplanar C_{2v}	minimum	−1000.24245	0
o-$C_6F_4(CO_2)_2^{2-}$	twisted C_2	minimum	−1000.21494	0

TABLE 2: Selected Optimized Parameters of $C_6X_5CO_2^-$ [a]

parameter	X = H	X = F
Bond Lengths (Å)		
C1−C6	1.411	1.381
C2−C5	1.409	1.377
C5−C6	1.407	1.380
C1−C12	1.555	1.566
C2−X9	1.097	1.325
C5−X10	1.098	1.326
C6−X11	1.095	1.324
C12−O14	1.265	1.221
Bond Angles (deg)		
C3−C1−C6	118.4	116.4
C4−C2−C5	119.2	119.3
C1−C6−X11	117.4	120.4
C5−C6−X11	121.7	117.2
C6−C5−X10	120.0	120.8
C2−C5−X10	119.7	119.5
O13−C12−O14	129.8	132.9

[a] For X = H, optimization is at the MP2 level of theory, and for X = F, optimization is at the HF level of theory.

TABLE 3: Selected Optimized Parameters of *p*-$C_6X_4(CO_2)_2^{2-}$ [a]

parameter	X = H	X = F
Bond Lengths (Å)		
C2−C5	1.413	1.381
C5−C6	1.409	1.381
C2−C14	1.548	1.555
C5−X9	1.096	1.337
C14−O16	1.271	1.229
Bond Angles (deg)		
C4−C2−C5	117.1	115.1
C2−C5−X9	117.5	119.8
C6−C5−X9	121.1	117.8
O15−C14−O16	127.9	130.5

[a] For X = H, optimization is at the MP2 level of theory, and for X = F, optimization is at the HF level of theory.

TABLE 4: Selected Optimized Parameters of *m*-$C_6X_4(CO_2)_2^{2-}$ [a]

parameter	X = H	X = F
Bond Lengths (Å)		
C1−C4	1.416	1.388
C2−C5	1.408	1.378
C4−C5	1.413	1.380
C4−C14	1.554	1.555
C1-X7	1.094	1.335
C5−X8	1.096	1.337
C2−X9	1.101	1.339
C14−O15	1.273	1.229
C14−O16	1.265	1.229
Bond Angles (deg)		
C3−C1−C4	121.9	125.1
C1−C4−C14	122.1	123.5
C5−C4−C14	119.4	120.8
C4−C5−X8	117.8	120.6
C2−C5−X8	121.9	117.4
C5−C2−C6	120.5	119.6
C4−C14−O15	115.6	114.8
C4−C14−O16	116.3	114.8

[a]For X = H, optimization is at the MP2 level of theory, and for X = F, optimization is at the HF level of theory.

***m*-$C_6H_4(CO_2)_2^{2-}$.** The meta isomer's minimum-energy structure (Figure 1c) is planar and has C_{2v} symmetry. Geometric parameters are given in Table 4.

***o*-$C_6H_4(CO_2)_2^{2-}$.** Optimizations on the ortho isomer that impose a planar C_{2v} geometry produce a structure with two imaginary frequencies. Reduction of the symmetry to C_s followed by optimization leads to the same C_{2v} structure. Another optimization was performed in C_{2v} symmetry by assuming that both carboxylate groups are rotated so that they are perpendicular to the ring plane. The resulting structure also has two imaginary frequencies. Only when both carboxylates are rotated out of the ring plane to produce a structure with C_2 symmetry is a minimum on the potential energy surface found. Data pertaining to this minimum are listed in Table 5. The dihedral angle between the carboxylate planes and the ring plane is approximately 52 °. The two C_{2v} structures mentioned above are 14.9 and 3.0 kcal/mol less stable than the minimum, respectively. Total energies pertaining to these structures are given in Table 6.

With zero-point vibrational energies included (see Table 6), the relative minimum energies of the three $C_6H_4(CO_2)_2^{2-}$ isomers place the para isomer lowest and the ortho isomer highest in energy. The para isomer is 28.9 kcal/mol lower than the ortho isomer and 4.9 kcal/mol lower than the meta isomer.

$C_6H_3(CO_2)_3^{3-}$. Optimizations on trianions failed to produce structures that are bound with respect to electron loss. The minimum energy conformation of the 1,3,5 isomer was found to have a planar D_{3h} structure whose HOMO was of E symmetry and had a Koopman's ionization energy of −0.5 eV.

$C_6F_5CO_2^-$. Geometry optimizations produce a C_{2v} structure in which the CO_2 group is perpendicular to the aromatic ring. Optimizations on a planar structure and subsequent frequency calculations show that this rotamer is a transition state that is 5.3 kcal/mol higher than the minimum-energy structure. Optimizations initiated with intermediate rotation angles lead to the C_{2v} minimum. Geometrical parameters for the minumum-energy structure are given in Table 7. The hydrogen analogue numbering scheme is used (Figure 1a).

***p*-$C_6F_4(CO_2)_2^{2-}$.** Optimization of this isomer leads to a minimum where both carboxylate groups are perpendicular to the central ring. Geometrical parameters are presented in Table 3. The hydrogen analogue numbering scheme is again used.

***m*-$C_6F_4(CO_2)_2^{2-}$.** Both carboxylate groups are perpendicular to the ring plane in the optimized structure. Geometrical parameters are presented in Table 4. The hydrogen analogue numbering scheme is again used. This isomer is 4.0 kcal/mol less stable than the para form (Table 5).

***o*-$C_6F_4(CO_2)_2^{2-}$.** The minimum-energy structure has two partially rotated carboxylate groups, which are rotated aproxi-

TABLE 5: Selected Optimized Parameters of *o*-$C_6X_4(CO_2)_2^{2-}$ [a]

parameter	X = H	X = F
Bond Lengths (Å)		
C1−C2	1.425	1.407
C1−C4	1.417	1.384
C4−C6	1.407	1.338
C5−C6	1.409	1.373
C4−X10	1.097	1.338
C6−X9	1.100	1.339
C1−C11	1.546	1.559
C11−O12	1.273	1.230
C11−O13	1.263	1.228
Bond Angles (deg)		
C2−C1−C11	126.4	125.5
C4−C1−C11	115.1	116.4
C1−C4−X10	117.2	121.2
C6−C4−X10	120.1	116.0
C5−C6−X9	120.7	119.9
C4−C6−X9	120.3	121.1
C1−C11−O12	115.0	114.3
C1−C11−O13	115.6	115.0

[a] For X = H, optimization is at the MP2 level of theory, and for X = F, optimization is at the HF level of theory.

TABLE 6: Zero-Point-Corrected Total Energies (au) and Energy Differences (kcal/mol) at the HF/aug-cc-pVDZ Level of Theory

isomer	*E*	Δ*E*
p-$C_6H_4(CO_2)_2^{2-}$	−604.70766	0
m-$C_6H_4(CO_2)_2^{2-}$	−604.69986	+4.9
o-$C_6H_4(CO_2)_2^{2-}$	−604.66167	+28.9
p-$C_6F_4(CO_2)_2^{2-}$	−1000.24888	0
m-$C_6F_4(CO_2)_2^{2-}$	−1000.24245	+4.0
o-$C_6F_4(CO_2)_2^{2-}$	−1000.21494	+21.3

TABLE 7: $C_6H_5CO_2^-$ VEDEs (eV)

symmetry	Koopman's	OVGF	pole strength
$3b_1$	5.38	5.11	0.89
$2a_2$	5.50	4.80	0.89
$1a_2$	5.80	5.07	0.89
$16a_1$	6.06	4.40	0.90
$11b_2$	6.20	4.57	0.90
$2b_1$	9.54	8.16	0.85

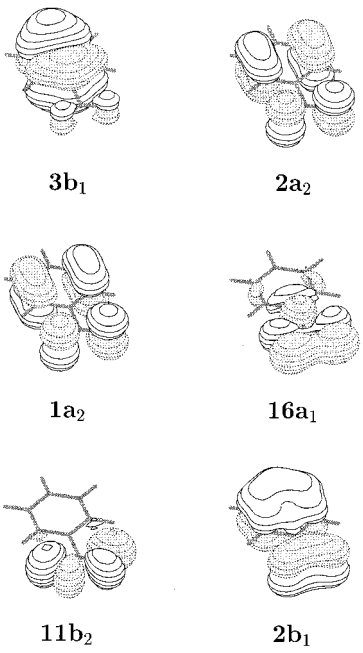

Figure 2. Dyson orbitals corresponding to the six highest occupied orbitals of $C_6H_5CO_2^-$.

mately 71° with respect to the plane of the aromatic ring. Geometrical parameters are presented in Table 5. The hydrogen analogue numbering scheme is again used. This isomer is the least stable, for it lies 21.3 kcal/mol above the para energy (Table 6).

$C_6F_3(CO_2)_3^{3-}$. Optimizations on trianions failed to produce structures that are bound with respect to electron loss. The minimum-energy conformation of the 1,3,5 isomer was found to be a nonplanar D_{3h} structure with the three carboxylate groups roated 90° with respect to the aromatic ring. The HOMO was of E symmetry and had a Koopman's ionization energy of −0.6 eV.

Electron Detachment Energies

$C_6H_5CO_2^-$. Electron propagator calculations on the vertical electron detachment energies (VEDEs) of the anion show the importance of electron correlation in describing the states of the neutral doublet. A complete reordering of the final states occurs between the Koopman's theorem and OVGF columns of Table 7. Propagator calculations of electron detachment energies converge with respect to energy in three iterations. All pole strengths are near 0.90. This value is indicative of the qualitative validity of the Koopman's picture and suggests that the OVGF model is likely to give reasonable results. Dyson orbitals corresponding to these results are shown in Figure 2. (Dyson orbital plots for the remaining seven structures are not presented in this work but are qualitatively similar to the anion and are discussed below.) Whereas Koopman's theorem predicts that an electron is removed from a ring-centered π level, OVGF results indicate that the lowest hole has oxygen lone pair character. The VEDE is 4.40 eV, qualifying the benzoate anion as a superhalide, for this value is larger than the electron affinities of all of the halogen atoms. It is likely that larger basis sets and more detailed treatments of electron correlation will produce larger electron binding energies. Another Dyson orbital, with b_2 symmetry (Figure 2), also is composed chiefly of oxygen lone pair lobes that lie in the plane of the nuclei. Three π levels follow at larger energies. Two a_2 Dyson orbitals are bonding and antibonding combinations of symmetry-adapted ring π and oxygen π patterns. The remaining level (b_1) originates primarily from a benzene π orbital.

TABLE 8: *p*-$C_6H_4(CO_2)_2^{2-}$ VEDEs (eV)

symmetry	Koopman's	OVGF	pole strength
$2b_{2g}$	2.07	1.42	0.89
$2b_{1g}$	2.31	1.79	0.89
$1a_u$	3.28	2.13	0.89
$1b_{1g}$	3.32	2.19	0.89
$11a_g$	3.63	1.92	0.90
$10b_{1u}$	3.66	1.93	0.89

In the Dyson orbital for the lowest VEDE, there is some delocalization onto the ring from the carboxylate group. The change in electron density on removal of an electron occurs primarily in the σ lone pair regions near the oxygen nuclei, but the exocyclic C−C bond will be weakened somewhat as well. This result is in accord with qualitative arguments that attach partial negative formal charges to the oxygens in a carboxylate group. The a_1 level is slightly above the b_2 level despite the O−O bonding relationships (bonding for a_1 and antibonding for b_2) because of destabilizing mixing with the nearby C−C bond-function lobe.

The largest shifts from canonical orbital energies to OVGF results are between 1.6 and 1.7 eV and are found for the two least-bound levels. Correlation corrections for the two a_2 Dyson orbitals are approximately 0.7 eV. A relatively small correction is obtained for the lowest b_1 case.

These patterns are typical of several classes of molecules with delocalized π systems and lone pair electrons. Examples include heterocyclic aromatics, p-element clusters, and certain kinds of organometallics. For heterocyclic aromatics, π and lone pair Dyson orbitals are usually misordered by Koopman's theorem results, and assignments based on calculations must include correlation effects. These corrections are usually minor for π orbitals, especially the HOMO. Lone pair character is associated with larger correlation corrections that reduce the predicted detachment energy, especially if the corresponding Dyson orbital is symmetric with respect to the nuclear plane.

***p*-$C_6H_4(CO_2)_2^{2-}$.** Electron detachment energies for the para isomer are shown in Table 8. The lowest detachment energy corresponds to a π level (b_{2g}) concentrated on the ring with minor destabilizing contributions from oxygen p orbitals. At a slightly higher energy, there is another benzene-like π orbital (b_{1g}). Oxygen contributions are even smaller because of the node that eliminates participation from carbon p orbitals in the exocyclic bond region. Correlation shifts are 0.65 and 0.52 eV for the b_{2g} and b_{1g} cases, respectively.

Much larger shifts are obtained for the σ lone pair levels. Although the corrections are approximately 1.7 eV for the a_g and b_{1u} Dyson orbitals, they are not large enough to surpass those of the π levels discussed above. The pattern of lobes around the carboxylate nuclei is similar to that found for the a_1 orbital of the monoanion. Because the two carboxylates are remote from each other, the two energies are similar.

Another pair of states corresponds to oxygen-centered π combinations. Correlation corrections here are only 1.1 eV, and the order of final states therefore is changed at the OVGF level of theory. Unlike the monoanion case (see the a_2 levels of the benzoate anion), there is little delocalization onto the ring. In one case, a_u, mixing of the oxygen-centered, symmetry-adapted combination of p orbitals can take place only with unoccupied π levels on the ring. Because of excess negative charge, this ring-centered π level is likely to be too destabilized to participate. In the b_{1g} case, mixing is permitted by symmetry with an occupied π level on the ring but is hardly seen in the orbital plot.

TABLE 9: *m*-$C_6H_4(CO_2)_2^{2-}$ VEDEs (eV)

symmetry	Koopman's	OVGF	pole strength
$3a_2$	2.10	1.48	0.89
$4b_1$	2.22	1.64	0.89
$2a_2$	3.10	1.96	0.89
$3b_1$	3.13	2.01	0.89
$16b_2$	3.24	1.53	0.90
$20a_1$	3.49	1.82	0.90

TABLE 10: *o*-$C_6H_4(CO_2)_2^{2-}$ VEDEs (eV)

symmetry	Koopman's	OVGF	pole strength
21b	1.66	0.79	0.89
22a	2.08	1.35	0.89
20b	2.44	1.25	0.89
21a	2.59	1.44	0.89
19b	2.71	1.01	0.90
20a	2.98	1.24	0.90

***m*-$C_6H_4(CO_2)_2^{2-}$.** Correlation plays a major role in the detachment energies of the meta isomer. Given the accuracy of the OVGF method (the average error is 0.25 eV), it is not possible to assign the order of the three lowest final states in Table 9 definitely. Only 0.16 eV separates the ring-centered π level with a_2 symmetry from its partner with b_1 symmetry. There is relatively little delocalization onto the oxygens in either of the Dyson orbitals. Correlation shifts are relatively small: 0.6 eV. Between these two states lies the b_2 level composed of oxygen-centered σ contributions. The correlation shift for the latter case, 1.7 eV, is relatively large. For the a_1 level, a 1.7-eV correlation shift is also obtained; the Dyson orbital exhibits a similar σ pattern, with the opposite phase relationship between the carboxylates. Shifts of 1.1 eV are obtained for the two oxygen-centered π lone pair levels. In the meta isomer, the carboxylate groups are still sufficiently distant to produce nearly identical detachment energies for the in-phase (b_1) and out-of-phase (a_2) combinations.

Correlation effects are similar in magnitude to the para case, given the composition of the corresponding Dyson orbitals. For the meta isomer, the first six states are compressed into a smaller energy range than they are for the para case: 0.53 versus 0.77 eV. Koopman's theorem results determine the chief differences between the meta and para isomers. At this level of theory, ring-centered π levels are the least bound, followed by oxygen-centered π levels and then by oxygen-centered σ levels. The closer proximity of the carboxylate groups in the meta isomer destabilizes the oxygen-centered lone pair levels of σ and π types. Ring-centered π levels are not affected to the same extent, which accounts for the narrower spread of the detachment energies.

***o*-$C_6H_4(CO_2)_2^{2-}$.** In the ortho isomer, there is no longer a plane of symmetry, but the pattern of orbital ordering at the Koopman's theorem level of theory (Table 10) remains the same. Before taking correlation into account, the two highest occupied orbital energies correspond to ring-centered π levels with some delocalization onto the oxygens. Lower symmetry allows the oxygen p orbitals to point more directly at the ring lobes. The resulting destabilization is more pronounced for the lowest b level because the ring-centered π fragment is more concentrated at the ring carbons nearest to the carboxylates than to its partner corresponding to the a representation. At the Koopman's theorem level, the splitting between the two states is 0.42 eV instead of 0.24 eV (para) or 0.12 eV (meta). Because of the enhanced antibonding relationships between the ring π and oxygen contributions, the lobes on the latter centers are somewhat larger than their counterparts in the para and meta isomers.

TABLE 11: $C_6F_5CO_2^-$ VEDEs (eV)

symmetry	Koopman's	OVGF	pole strength
$9b_1$	6.22	4.94	0.90
$4a_2$	6.51	5.42	0.90
$24a_1$	6.76	5.70	0.90
$3a_2$	6.86	5.03	0.90
$8b_1$	7.71	6.26	0.90
$15b_2$	11.10	9.48	0.88

TABLE 12: *p*-$C_6F_4(CO_2)_2^{2-}$ VEDEs (eV)

symmetry	Koopman's	OVGF	pole strength
$6b_{2g}$	2.66	1.42	0.90
$3b_{3g}$	3.11	1.97	0.90
$2a_u$	3.88	2.75	0.89
$2b_{3g}$	3.90	2.75	0.89
$14a_g$	4.10	2.27	0.90
$13b_{3u}$	4.20	2.34	0.90

Correlation shifts in the detachment energies are similar in magnitude to those that occur in the other isomers. The order of the final states is changed once again. Two oxygen-centered lone pair levels with some delocalization into the ring σ region have 1.7-eV correlation corrections, whereas two other oxygen lone pair levels with virtually no ring contributions have 1.1-eV correlation shifts. A 0.7-eV correction is found for the ring-centered level belonging to the totally symmetric representation. All of these changes at the OVGF level bear close resemblance to the para and meta results. Only for the lowest detachment energy is there a notable change in the correlation effect. In this case, the shift is closer to 0.9 eV.

The lowest detachment energy for the ortho isomer is notably lower than its para and meta counterparts. A smaller separation between the carboxylate groups destabilizes all canonical orbital energies and OVGF detachment energies for this isomer. This destabilization is especially large for the highest occupied orbital because the ortho − meta difference for the lowest b detachment energy at the Koopman's theorem level is 0.56 eV. The corresponding difference for the lowest detachment energy is only 0.02 eV. The larger correlation effect for the lowest detachment energy accentuates the contrast.

$C_6F_5CO_2^-$. Ionization energies are given in Table 11. The lowest ionization energy, 4.94 eV, is definitely higher than the value pertaining to $C_6H_5CO_2^-$ (4.40 eV). The corresponding Dyson orbital exhibits extensive delocalization and antibonding relationships between one of the ring's π orbitals and contributions from the F atoms and the rotated carboxylate group. Oxygen p orbitals on the carboxylate group are pointed directly at the ring's π lobes.

***p*-$C_6F_4(CO_2)_2^{2-}$.** The lowest electron detachment energy of Table 12, 1.42 eV, is almost identical to its counterpart for $C_6H_4(CO_2)_2^{2-}$. Delocalization over the ring, F atoms, and carboxylate oxygens is seen in the Dyson orbital, and antibonding relationships are obtained between the ring and substituent lobes.

***m*-$C_6F_4(CO_2)_2^{2-}$.** Fluorination increases the lowest electron detachment energy at the Koopman's level, but correlated results show only a slight increase: 1.51 versus 1.48 eV (Tables 9 and 13). In the Dyson orbital, a similar pattern of delocalization and antibonding relationships between ring and substituent lobes is present. There is a slight polarization of the ring π contribution toward the carboxylates and away from the fluorides.

***o*-$C_6F_4(CO_2)_2^{2-}$.** Substitution of F for H substituents causes the VEDE to increase from 0.79 to 1.11 eV (Tables 10 and 14). The pattern of phase relationships and delocalization in the Dyson orbital is compatible with the precedents of the para and meta isomers. Polarization of the ring π contribution toward

TABLE 13: *m*-$C_6F_4(CO_2)_2^{2-}$ VEDEs (eV)

symmetry	Koopman's	OVGF	pole strength
$7a_2$	2.74	1.51	0.90
$10b_1$	2.88	1.66	0.90
$6a_2$	3.72	2.57	0.90
$9b_1$	3.72	2.56	0.90
$18b_2$	3.72	1.88	0.90
$24a_1$	4.25	2.42	0.90

TABLE 14: *o*-$C_6F_4(CO_2)_2^{2-}$ VEDEs (eV)

symmetry	Koopman's	OVGF	pole strength
29b	2.43	1.11	0.90
30a	2.85	1.61	0.90
28b	3.02	1.28	0.90
29a	3.06	1.83	0.90
27b	3.18	1.85	0.90
28a	3.68	1.81	0.90

TABLE 15: ΔHF Electron Detachment Energies (eV)

structure	vertical	adiabatic
$C_6H_5CO_2^-$	4.078	3.826
p-$C_6H_4(CO_2)_2^{2-}$	0.742	0.420
m-$C_6H_4(CO_2)_2^{2-}$	0.694	0.413
o-$C_6H_4(CO_2)_2^{2-}$	0.067	0.008

the carboxylates and away from the fluorides takes place to a greater extent in this isomer.

Adiabatic Electron Detachment Energies

The three hydrogen-containing dianions studied were found to have relatively small VEDEs, especially the ortho isomer (1.42, 1.48, and 0.79 eV respectively). Calculation of the adiabatic electron detachment energies (AEDE) is necessary to ensure that these species are indeed stable to loss of an electron. Vertical and adiabatic electron detachment energies were calculated using the total energy difference method for the four hydrogen-containing species. These results are summarized in Table 15. $C_6H_5CO_2^-$ is found to have a VEDE of >4.0 eV and an AEDE of >3.8 eV. Meta and para $C_6H_4(CO_2)_2^{2-}$ isomers have much smaller VEDEs and AEDEs, averaging around 0.7 and 0.4 eV, respectively. The VEDE and AEDE values for ortho $C_6H_4(CO_2)_2^{2-}$ are even smaller, the AEDE being near zero.

VEDEs obtained using propagator methods have several advantages over VEDEs obtained using the energy difference method, including the fact that the energy difference method involves finding a small difference between two very large total energies. The difference between the VEDE and the AEDE is sometimes called the relaxation energy or the reorganization energy. The relaxation energies obtained from the energy difference method can be combined with the more accurate VEDEs obtained using the propagator methods to arrive at better estimates of the AEDEs. $C_6H_5CO_2^-$ then has an estimated AEDE of 4.15 eV. The para, meta, and ortho isomers of $C_6H_4(CO_2)_2^{2-}$ have AEDEs of 1.16, 1.20, and 0.73 eV, respectively.

Charge Delocalization

The unusually large VEDE of $C_6H_5CO_2^-$ is large enough to qualify it as a superhalide. It is of interest to consider why this species and to a lesser extent why the other aromatic anions exhibit such large VEDEs. One explanation may be that conjugation between the carboxylate group and the aromatic ring allows for a large amount of charge delocalization over the molecule. Examination of the highest molecular orbitals shows that several of them are dominated by contributions from orbitals centered on the aromatic ring.

TABLE 16: Selected Properties of $C_6H_5CO_2$ and $C_6F_5CO_2$

structure	Z_{CO_2}	Z_{ring}	Koopman's IP (eV)
planar $C_6H_5CO_2^-$	−1.05	+0.05	5.38
nonplanar $C_6H_5CO_2^-$	−1.20	+0.20	4.98
planar $C_6H_5CO_2$	−0.91	+0.91	10.48
planar $C_6F_5CO_2^-$	−0.75	−0.25	6.33
nonplanar $C_6F_5CO_2^-$	−0.91	−0.08	6.22

One way to try to quantify this effect is to consider the partial atomic charges as obtained from a Mulliken population analysis. Table 16 gives a summary of the partial atomic charges as well as Koopman's approximation of the ionization energy for $C_6H_5CO_2^-$ in its planar form, the transition state corresponding to the carboxylate group rotated 90° with respect to the aromatic ring and the planar $C_6H_5CO_2$ neutral radical. In all three cases, the structure has been fully optimized. Z_{CO_2} is the sum of the partial atomic charges of the three atoms comprising the carboxyate group, whereas Z_{ring} is the sum of the partial atomic charges of the ring carbon and hydrogen atoms.

Upon rotation of the anion from the planar to the nonplanar conformation, the sum of the charges on the carboxylate atoms decreases by 0.15, whereas the charge on the ring increases by the same amount. The Koopman's VEDE is also seen to decrease by 0.4 eV. It appears that the rotation of the carboxylate group reduces the conjugation of the ring with the carboxylate group, resulting in greater localization of charge on the carboxylate group, which could increase the electron−electron repulsion and thereby reduce the VEDE.

When removing an electron from the planar anion and obtaining the planar radical neutral structure, the sum of the charges on the carboxylate atoms decreases by just 0.14, whereas the sum of the charges on the ring atoms decreases by 0.86. Thus, in the ionization process, at least for the HOMO predicted by Koopman's ordering, the majority of the charge density is lost from the aromatic ring rather than from the carboxylate group.

The situation is somewhat similar in the case of $C_6F_5CO_2$. Upon rotation of the carboxylate group from the planar to the nonplanar conformation, the partial charge on the carboxylate group increases in magnitude from −0.75 to −0.91, whereas the Koopman's ionization energy decreases from 6.33 to 6.22 eV. However, it is the nonplanar conformation that is lower in energy. The fluorine-containing species in its nonplanar conformation still has higher VEDEs than does the hydrogen analogue in its planar conformation. Comparison of the amount of charge on the carboxylate group between the hydrogen and fluorine species when both are in the nonplanar conformation shows that the fluorine analogue has a partial charge that is lower in magnitude (−1.20 vs −0.91). Thus, the highly electronegative fluorine atoms appear to allow a greater portion of the excess charge to reside on the ring portion of the molecule, which reduces the electron−electron repulsion and results in an increased VEDE.

Conclusions

The VEDE of the benzoate anion determined by electron propagator calculations, 4.4 eV, qualifies this species as an organic superhalide. To identify the correct final state in this detachment, it is necessary to account for electron correlation. Correlation corrections to VEDEs corresponding to Dyson orbitals with O-centered σ lone pair contributions are larger than those for the ring-centered π Dyson orbitals. The order of the

neutral final states therefore changes from Koopman's theorem to OVGF. For the lowest VEDE, the corresponding Dyson orbital is dominated by O-centered σ lone pairs destabilized by delocalization into the exocyclic C−C bond region.

Geometry optimizations on $C_6H_4(CO_2)_2^{2-}$ yield planar minima for the para and meta cases, but the ortho minimum has rotated carboxylate groups such that a C_2 axis of symmetry remains. The rotation barrier for a single carboxylate in the para isomer is 5.6 kcal/mol. Rotation of both carboxylates in the ortho isomer such that they are perpendicular to the aromatic ring requires 3.0 kcal/mol. The para isomer is the most stable and the ortho isomer is least stable of the three.

VEDEs for the para and meta isomers of the dianion are 1.4 eV and are 0.8 eV for the ortho isomer. In the uncorrelated picture, ring-centered π orbitals are highest in energy, followed by O-centered π and O-centered σ orbitals. Destabilization of the ring-centered π levels by antibonding interactions with oxygen contributions is more pronounced in the dianions than in the monoanion. Correlation effects in the electron detachment energies of dianions change the order of the final states but do not affect the identification of the lowest final state. These corrections lower all detachment energies, but the shifts are larger for the O-centered levels, especially those with σ patterns.

Perfluorinated monoanions and dianions have larger electron detachment energies than their hydrogenated counterparts. Differences between these species are especially significant in the case of the mononanion, where the lowest detachment energy is 4.9 eV. For the dianions, only in the ortho case is there a substantial increase in the VEDE after F substitution for H. Equilibrium geometries for the monoanion and the dianions feature carboxylate groups that are perpendicular or, in the case of the ortho dianion, partially rotated with respect to the aromatic ring's plane. Dyson orbitals corresponding to the lowest electron detachment energies are composed chiefly of ring π orbitals, but there is substantial delocalization onto the F and carboxylate regions. Antibonding interactions with F π and oxygen p orbitals directed toward the ring π lobes also characterize these Dyson orbitals.

Acknowledgment. Dr. V. G. Zakrewski of Kansas State University and Dr. E. Walters of The University of New Mexico provided extensive advice for this project.

References and Notes

(1) Dreuw, A.; Cederbaum, L. S. *Chem. Rev.* **2002**, *102*, 181.
(2) Gutsev, G. L.; Boldyrev, A. I. *Chem. Phys.* **1981**, *56*, 277.
(3) Gutsev, G. L.; Boldyrev, A. I. *Adv. Chem. Phys.* **1985**, *61*, 169.
(4) Scheller, M.; Cederbaum, L. *J. Chem. Phys.* **1993**, *99*, 441.
(5) Gutowski, M.; Boldyrev, A.; Ortiz, J. V.; Simons, J. *J. Am. Chem. Soc.* **1994**, *101*, 9262.
(6) Scheller, M.; Cederbam, L. *Chem. Phys. Lett.* **1993**, *216*, 141.
(7) Watts, J.; Bartlett, R. J. *J. Chem. Phys.* **1992**, *97*, 3445.
(8) Zakrzewski, V. G.; Ortiz, J. V. *J. Chem. Phys.* **1995**, *102*, 294.
(9) Sommerfield, T.; Scheller, M. K.; Cederbaum, L. S. *Chem. Phys. Lett.* **1993**, *209*, 216.
(10) Enlow, M. A.; Ortiz, J. V.; Luthi, H. P. *Mol. Phys.* **1997**, *92*, 441.
(11) Frisch, M. J.; Trucks, G. W.; Schlegel, H. B.; Gill, P. M. W.; Johnson, B. G.; Robb, M. A.; Cheeseman, J. R.; Keith, T.; Petersson, G. A.; Montgomery, J. A.; Raghavachari, K.; Al-Laham, M. A.; Zakrzewski, V. G.; Ortiz, J. V.; Foresman, J. B.; Cioslowski, J.; Stefanov, B. B.; Nanayakkara, A.; Challacombe, M.; Peng, C. Y.; Ayala, P. Y.; Chen, W.; Wong, M. W.; Andres, J. L.; Replogle, E. S.; Gomperts, R.; Martin, R. L.; Fox, D. J.; Binkley, J. S.; Defrees, D. J.; Baker, J.; Stewart, J. P.; Head-Gordon, M.; Gonzalez, C.; Pople, J. A. *Gaussian 94*, revision D.3; Gaussian, Inc.: Pittsburgh, PA, 1995.
(12) Dunning, T. H., Jr. *J. Chem. Phys.* **1989**, *90*, 1007.
(13) Kendall, R. A.; Dunning, T. H., Jr.; Harrison, R. J. *Chem. Phys.* **1992**, *96*, 6796.
(14) Cederbaum, L. S. *J. Phys. B: At. Mol. Opt. Phys.* **1975**, *8*, 290.
(15) von Niessen, W.; Schirmer, J.; Cederbaum, L. S. *Comput. Phys. Rep.* **1984**, *1*, 57.
(16) Zakrzewski, V. G.; Ortiz, J. V. *Int. J. Quantum Chem., Quantum Chem. Symp.* **1994,** *28*, 23.
(17) Zakrzewski, V. G.; Ortiz, J. V. *Int. J. Quantum Chem.* **1995**, *53*, 583.
(18) Schaftenaar, G. *MOLDEN*; CAOS/CAMM Center: The Netherlands, 1991.